SMAR 2015 – Third Conference on Smart Monitoring,
Assessment and Rehabilitation of Civil Structures

SMAR 2015

Performance of Superelastic Shape Memory Alloy Reinforced Concrete Members

Dan Palermo[1], Alaa Abdulridha[2], and Wilmar Leonardo Cortes Puentes[3]

[1] Department of Civil Engineering, York University, Toronto, Canada
[2] Department of Civil Engineering, University of Ottawa, Ottawa, Canada
[3] Department of Civil Engineering, University of Ottawa, Ottawa, Canada

ABSTRACT: The focus of this paper is to present experimental results of a concrete beam and slender concrete shear wall reinforced internally with Superelastic (SE) Shape Memory Alloy (SMA) bars. In addition, preliminary results of a novel SE-SMA brace proposed for external retrofitting of reinforced concrete structural elements will be presented. The beam tests presented herein were part of a study that assessed the performance of SMA reinforced members subjected to various loading conditions, including: monotonic, cyclic, and reverse cyclic. The slender shear wall testing demonstrated the performance of lateral force resisting members reinforced with a hybrid of SE-SMA and traditional deformed reinforcing steel within the plastic hinge region. Preliminary results of the proposed SE-SMA brace demonstrate promise for upgrading the performance of seismically deficient structural members. Due to the large recoverable strain capacity of SE-SMAs, the brace has the potential of being reused after the structure experiences a seismic event.

1 INTRODUCTION

The application of Shape Memory Alloys (SMAs) in civil engineering applications is in its infancy. The capacity of Superelastic (SE) Shape Memory Alloys (SMAs) to recover large strains upon removal of loading is a unique mechanical property that makes them appealing for seismic applications. The recoverable strains are in the range of 6%, after which permanent straining begins to accumulate. In contrast, the recoverable strains in traditional reinforcing steels are in the range of 0.2%. Therefore, SMAs have potential applications in developing novel self-centering structures. Such structures are envisioned to restore to their original state after a seismic event. In addition, SMAs are characterized as providing energy dissipation through hysteretic damping, as having strength comparable to traditional reinforcing steel, and as being highly corrosion resistant. Conversely, some of the shortcomings of SMAs are their high cost, dependency of the superelastic properties on operating temperature, smooth bar surface, and low elastic modulus.

Recent studies have investigated SE-SMAs as internal reinforcement in concrete structural members. Deng et al (2006) studied concrete beams reinforced with SMA wires, Saiidi and Wang (2006) investigated concrete columns reinforced with SMAs in the plastic hinge region, Saiidi et al (2009) focused on concrete columns reinforced with SMAs and engineering cementitious concrete, Youssef et al (2008) investigated a beam-column joint reinforced with SMAs in the plastic hinge regions, and Abdulridha et al (2013) studied beams reinforced with SMAs in the critical region. These experimental studies have demonstrated the effectiveness of SE-SMA reinforced concrete structural elements to recover large imposed deformations highlighting the self-centering capacity of SMAs. External applications of SE-SMAs have also been reported by Effendy et al (2006). While advancements have been made by each of these studies, additional experimental testing is required to further demonstrate the applicability of SMA reinforced concrete components.

2 EXPERIMENTAL TESTING

Experimental test results of one reinforced concrete beam and one slender shear wall reinforced with SMA longitudinal bars will be presented. Furthermore, preliminary results of an SMA brace for external retrofitting will be discussed. The SMA bars used in the following test programs had a smooth surface and consisted of Nickel-Titanium (NiTi).

2.1 SMA reinforced concrete beam

A series of tests was conducted to assess the performance of beams reinforced longitudinally with SMA bars in comparison to beams reinforced with traditional deformed steel. Seven beam tests were conducted. One SMA-reinforced and one steel-reinforced beam formed a companion pair. The companion beams were subjected to one of the following loading protocols: monotonic, cyclic, or reverse cyclic. A seventh test was conducted to subject an SMA beam to monotonic loading. For brevity, only the SMA- (B6-NR) and steel-reinforced (B3-SR) beams subjected to reverse cyclic loading will be presented. Detailed results of the other beam tests can be found elsewhere (Abdulridha et al 2013).

The beams were 2800 mm in total length, 125 mm in width, and 250 mm in depth. The length of the beams spanning from center-to-center of the supports was 2400 mm. The two beams were doubly reinforced. Beam B3-SR contained 2-10M deformed longitudinal bars (100 mm^2 and 11.3 mm diameter) at the top and bottom. Beam B6-NR contained 2-12.7 mm diameter SMA (NiTi) longitudinal bars at the top and bottom over a length of 600 mm centered at the midspan. The SMA bars were coupled to 15M deformed bars (200 mm^2 and 16 mm diameter) that extended to the ends of the beam. Standard threaded mechanical couplers were used. The SMA bars were reshaped to a diameter of 9.5 mm over a length of 300 mm at the center to prevent rupture of the SMA bars at the coupler where the bars were threaded. Both beams were reinforced with smooth 6.35 mm diameter closed stirrups over the entire length of the beam. The stirrups were spaced at 100 mm. The concrete clear cover was 20 mm. The yield strengths were 425 MPa and 415 MPa for the 10M steel and 12.7 mm SMA bars, respectively, while the respective ultimate strengths were 615 MPa and 800 MPa. Note that the ultimate strength of the SMA bars is based on specifications provided by the manufacturer. On the day of testing, the compressive strength of the concrete was 34.6 MPa and 32.7 MPa for Beams B3-SR and B6-NR, respectively. Figure 1 provides the cyclic stress-strain response of the 10M steel and 12.7 mm SMA bars, while Figure 2 is a photo of one of the beams prior to testing.

The beams were tested under a similar loading protocol following displacement control. In the pre-yield phase, the beams were subjected to midspan displacements of $0.33\Delta y$ to $1.0\Delta y$ in increments of $0.33\Delta y$. In the post-yield regime, loading was imposed in increments of $1.0\Delta y$ until failure. Yield displacements of 6.4 mm and 5.7 mm were determined for the SMA- and steel-reinforced beams, respectively, using the results of beam tests subjected to monotonic loading (Abdulridha et al 2013).

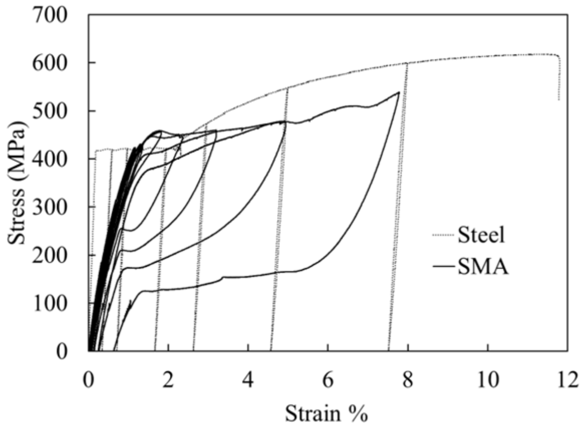

Figure 1. Cyclic stress-strain response of 10M and SMA reinforcing bars.

Figure 2. Beam prior to testing.

Figures 3 a) and b) provide the normalized load-displacement ductility responses of Beams B3-SR and B6-NR, respectively. The load was normalized by the yield strength (*Asfy*) of the longitudinal reinforcement to account for differences in yield stress and bar area, while the midspan displacement is reported as displacement ductility (Δ/Δ_y) to include the differences in yield displacement.

The responses bring to light similarities and differences in behavior. The normalized yield and peak loads were 0.32 (27 kN) and 0.41 (35 kN), respectively, for Beam B3-SR and 0.34 (20 kN) and 0.39 (23 kN), respectively, for Beam B6-NR. The ductility was 9.4 and 9.5, respectively, for B3-SR and B6-NR. Therefore, the steel-reinforced (B3-SR) and the SMA-reinforced (B6-NR) beams experienced similar normalized yield and peak loads, and ductility. Notable differences are the displacement recovery and energy dissipation capacities. At the ultimate displacement ductility, Beam B6-NR recovered 85% of the imposed midspan displacement, while B3-SR recovered only 26%. This significant difference is directly attributed to the behavior of the longitudinal reinforcement. The SMA bars were effective at restoring the beam, while the traditional deformed reinforcement experienced accumulation of permanent straining with increased loading. This recovery of the SMA bars resulted in a pinched behavior in the load-displacement responses. As a result, Beam B6-NR dissipated 1205 kN mm of energy, while B3-SR dissipated 3345 kN mm of energy at the ultimate displacement ductility. The energy dissipated by Beam B6-NR was lower, mostly owing to the pinched behavior, and to a lesser extent the slightly lower tensile yield force capacity of the SMA bars. Beam B3-SR experienced a typical flexural failure involving yielding of the longitudinal reinforcement and crushing of the compression concrete at midspan. Beam B6-NR failed due to rupturing of the SMA bar at the transition zone where the bar diameter changed from 9.5 mm to 12.7 mm.

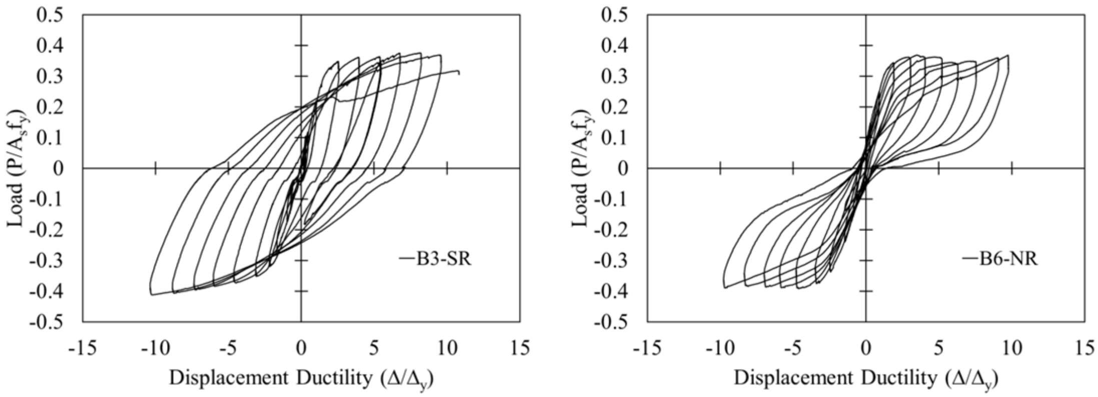

(a) (b)

Figure 3. Normalized load-displacement ductility responses: (a) Beam B3-SR; and (b) Beam B6-NR.

2.2 *SMA reinforced shear wall*

An experimental study was conducted on a slender shear wall (W2-NR) reinforced in the boundary elements with SMAs as the principal reinforcement (Abdulridha 2013). All other reinforcement consisted of traditional deformed steel, resulting in an SMA-hybrid wall. A companion wall (W1-SR) consisting of only deformed steel was also constructed. The walls were 2200 mm in height, 1000 mm in length, and 150 mm in thickness, and were designed according to ductile requirements according to the Canadian Standards Association (CSA) A23.3 Design of Concrete Structures (2004). The web portion of the wall contained two curtains of vertical and horizontal 10M deformed bars spaced at 150 mm. The boundary zone of W1-SR was reinforced with 4-10M longitudinal bars; while in W2-NR the longitudinal reinforcement consisted of 4-12.7 mm diameter SMA bars. The SMA bars were used over a length of 950 mm from the base of the wall and were coupled to 15M deformed bars. Anti-buckling ties were also used in the boundary zones and spaced at 75 mm within the plastic hinge region and 150 mm above this zone. Furthermore, four pairs of 10M bars were placed within the web to increase the sliding shear resistance. These starter bars extended 300 mm into the wall. The yield strength of the SMA and 10M was 380 and 425 MPa, respectively. The ultimate strength of the 10M bar was 615 MPa, while the manufacturer specified ultimate strength of the SMA was 1068 MPa. The compressive strength of the concrete on the day of testing was 30.5 MPa and 31.6 MPa, respectively for Walls W1-SR and W2-NR. Figure 4 is a photo of Wall W2-NR prior to testing.

Figure 4. Shear wall W2-NR prior to testing.

The shear walls were subjected to reverse cyclic displacements imposed along the top loading beam. Figure 5 provides the lateral load-drift responses of the two walls. Note that the drift was based on the displacements imposed at the mid height of the top loading beam relative to the base of the wall; a height of 2400 mm.

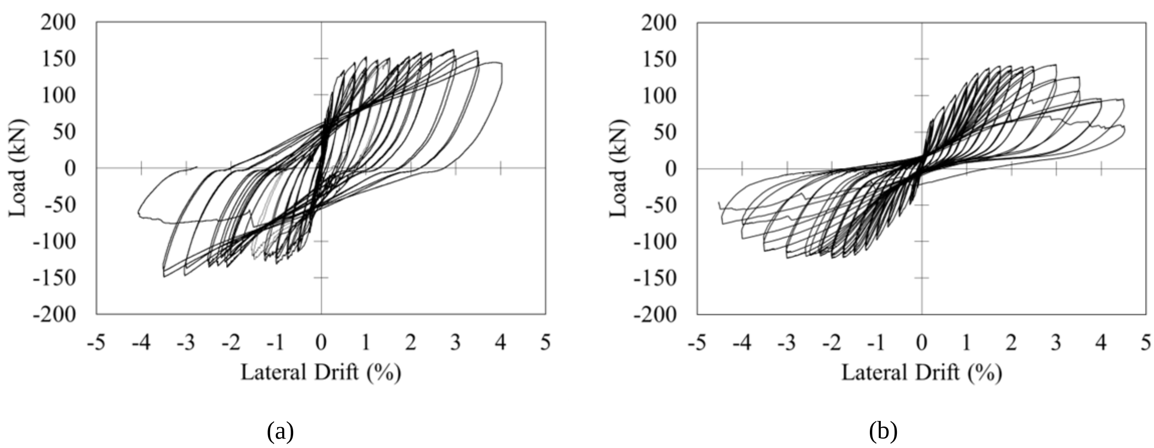

Figure 5. Lateral load-drift responses: a) Wall W1-SR; and b) Wall W2-NR

Wall W1-SR yielded at 116 kN of load corresponding to a drift of 0.39% (9.4 mm), while Wall W2-NR yielded at 112 kN at a drift of 1.1% (26.4 mm). Yielding was based on an equivalent elasto-plastic system with a secant stiffness passing through the load-displacement response at 75% of the average nominal lateral strength. [Note that the yield load and drift were based on an average between the positive and negative loading directions.] While the yield loads are similar, the corresponding drifts differ substantially. This is attributed to the significantly lower modulus of the SMA (38 GPa) compared to the deformed steel (205 GPa). The average secant stiffness at yielding was 12.34 kN/mm and 4.24 kN/mm for Walls W1-SR and W2-NR, respectively. The average peak lateral load was 156 kN, which was sustained at 3.2% drift (76 mm) for W1-SR; while W2-NR experienced a peak load of 133 kN at a drift of 3% (72 mm). Wall W1-SR failed at approximately 3.9% drift in the negative direction of loading due to rupturing of the exterior principal reinforcement in the boundary zone. This was accompanied with concrete crushing in the opposite boundary zone. Wall W1-SR maintained the lateral load capacity up to a drift of

3.5%. Conversely, Wall W2-NR experienced a number of drops in the lateral load capacity. This was attributed to rupturing of the vertical reinforcement in the web reinforcement while the SMA bars in the boundary zone remained intact. Fracturing of the web vertical reinforcement was first noted during the second repetition of loading to a drift of 3%. Fracturing occurred at a distance of approximately 350 mm above the base of the wall, slightly above the termination point of the starter bars and coincident with one of the major horizontal cracks that surfaced in the wall. After concrete was removed from the lower portion of the W2-NR, it became evident that one of the SMA bars fractured at the location of the couplers, approximately 800 mm above the base of the wall. Therefore, the drift capacity of Wall N2-NR was controlled by fracturing of the deformed steel in the web. It is probable that using SMA bars for the vertical reinforcement throughout the wall would have resulted in higher drift capacity. Figure 6 illustrates damage that was sustained by Walls W1-SR and W2-NR at the end of testing.

(a) (b)

Figure 6. Condition of walls at the end of testing: a) Wall W1-SR; and b) Wall W2-NR

The cracking sustained by the walls was markedly different. Wall W1-SR was typical of well distributed cracking throughout the wall that is characteristic of structural elements reinforced with closely spaced deformed reinforcement. Conversely, cracking in W2-NR was spaced significantly farther. This is attributed to the smooth bar surface of the SMA. Heavy damage was experienced by both walls near the termination point of the starter bars. The starter bars shifted the critical section away from the base of the wall.

2.3 External SMA bracing

Research has commenced at exploiting SMAs as external bracing for structural components. Such braces can be used as a retrofitting methodology or as braces in new construction. Figure 7 illustrates a proposed tension-only SMA brace for retrofitting seismically deficient reinforced concrete shear walls (Cortés-Puentes and Palermo 2015). The proposed brace consists of two HSS 50 mm x 50 mm x 4 mm rigid steel elements that are coupled with one, 635 mm-long, 12.7 mm-diameter SMA bar. The SMA bar is connected to two screw-lock couplers, one at each end of the SMA bar. Tension-only response is achieved by welding one of the couplers to a stiff steel assembly while the other end is free to move through the stiff end assembly. The end assemblies, in turn, are bolted to the rigid HSS elements. The SMA bar is sized to ensure that it remains within its superelastic strain recovery limit (6%).

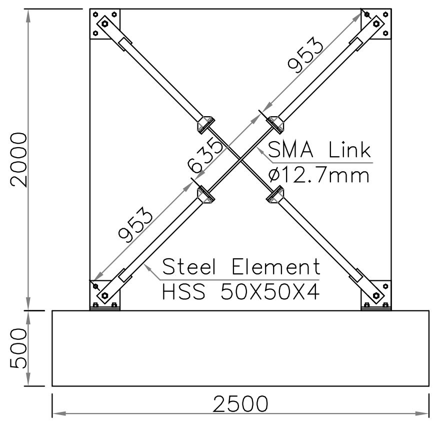

Figure 7. Application of proposed SMA brace for retrofitting deficient structural members.

Figure 8 is a photo of the proposed SMA brace during axial load testing. The brace was connected to a rigid block at one end and to a hydraulic actuator at the other end. The intent of the bare brace test was to establish the cyclic response for numerical modelling and to test the individual brace components.

Figure 8. Proposed SMA brace subjected to cyclic loading.

Figure 9 provides the axial load-elongation of the proposed SMA brace from testing conducted as illustrated in Figure 8. The target elongation during testing was 35 mm, corresponding to approximately 5.5% strain in the SMA bar. Two repetitions of loading were imposed on the brace. The response demonstrates the capacity of the brace to return to its original length. The maximum permanent elongation was 2.5 mm corresponding to a strain of 0.1%. The SMA ruptured at 41 mm of elongation adjacent to one of the end couplers. A subtle characteristic of the SMA brace was the near similar hysteretic response (strength, stiffness, and energy dissipation) between the first and second repetition of loading, which is attributed to the re-centering capacity of the SMA bar. Conversely, a tension-only brace incorporating a deformed steel bar would result in significant differences between the two repetitions of loading. The first loading cycle would result in a wide hysteretic response as a result of large permanent elongation. However, the second repetition of loading would be substantially narrower with marginal energy dissipation.

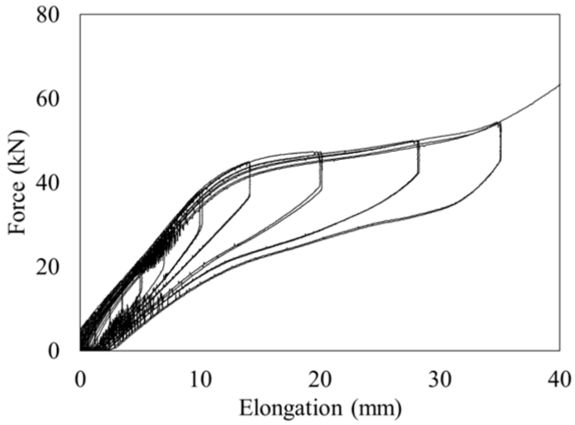

Figure 9. Force-elongation response of tension-only SMA brace.

3 CONCLUSIONS

Results of an SMA reinforced beam and slender shear wall, and preliminary results of a proposed external SMA bracing system were presented in this paper. The SMA reinforced beam and shear wall demonstrated the capacity of the member to recover significant nonlinear displacements, sustain comparable yield and ultimate load capacities, and ultimate displacement capacities to companion steel-reinforced members. Notable differences included the lower initial stiffness of the SMA members and energy dissipation capacities relative to the steel reinforced members. The proposed tension-only SMA bracing system also demonstrated the capacity of the SMA to restore large imposed deformations.

4 REFERENCES

Abdulridha, A., 2013, Performance of superelastic shape memory alloy reinforced concrete elements subjected to monotonic and cyclic loading. *Ph.D. Thesis*, University of Ottawa, Ottawa, Canada.

Abdulridha, A., Palermo, D., Foo, S., and Vecchio, F.J., 2013, Behavior and modeling of superelastic shape memory alloy reinforced concrete beams. *Engineering Structures*, 49: 893-904.

Canadian Standards Association A23.3-04, 2004, Design of concrete structures. *Canadian Standards Association*, Rexdale, Ontario, Canada.

Cortés-Puentes, W. L., and Palermo, D., 2015, Tension-only SMA bracing for seismic retrofitting. *Fifth International Conference on Construction Materials (CONMAT'15)*, Whistler, Canada

Deng Z, Li Q, and Sun H., 2006, Behaviour of concrete beam with embedded shape memory alloy wires. *Engineering Structures*, 28: 1691–1697.

Effendy E., Liao W., Song G., Mo Y., Loh C., 2006, Seismic behaviour of low-rise shear walls with SMA bars. *Earth & Space: engineering, construction, and operations in challenging environment*, Houston, TX.

Saiidi, M. S., and Wang. H., 2006, Exploratory study of seismic response of concrete columns with shape memory alloys reinforcement. *ACI Structural Journal*, 103(3): 436-443.

Saiidi M. S., O'Brien M., Sadrossadat-Zadeh M., 2009, Cyclic response of concrete bridge columns using superelastic nitinol and bendable concrete. *ACI Structural Journal*, 106(1): 69–77.

Youssef, M., Alam, M., and Nehdi, M., 2008, Experimental investigation on the seismic behaviour of beam-column joints reinforced with superelastic shape memory alloys. *Journal of Earthquake Engineering*, 12: 1205-1222.